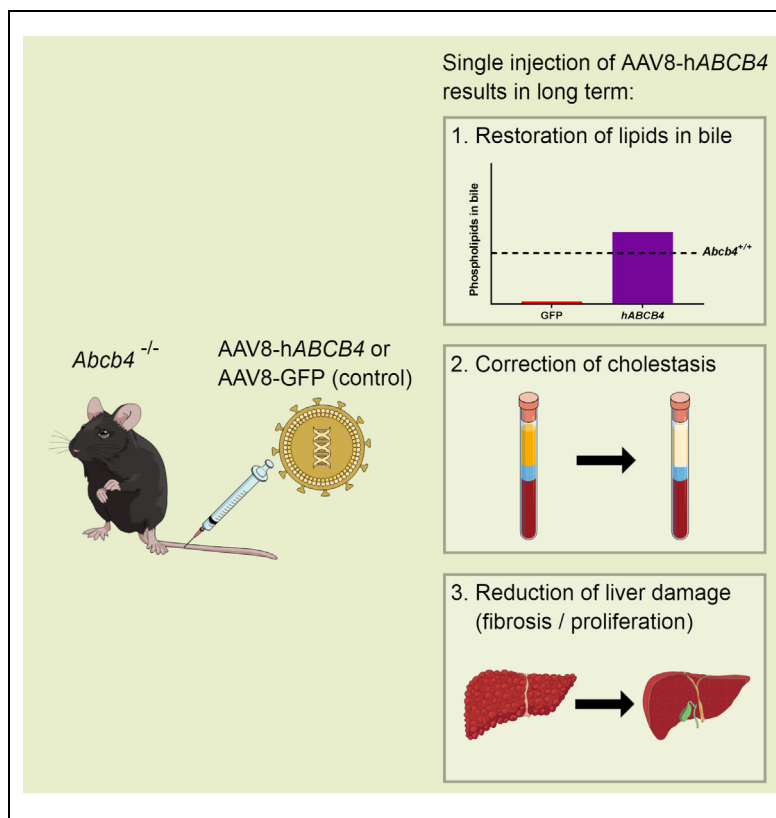


# Liver-directed gene therapy results in long-term correction of progressive familial intrahepatic cholestasis type 3 in mice

## Graphical abstract



## Highlights

- Adeno-associated virus (AAV)-mediated gene therapy can correct *Abcb4* deficiency (PFIC3) in mice.
- By restoring phospholipid transport to bile, cholestasis and liver damage were strongly reduced.
- Stable transgene expression resulted in long-term correction of the phenotype (26 weeks).
- Hepatic transgene persistence was achieved by sufficiently reducing hepatocyte proliferation.

## Authors

Sem J. Aronson, Robert S. Bakker, Xiaoxia Shi, ..., Ulrich Beuers, Coen C. Paulusma, Piter J. Bosma

## Correspondence

p.j.bosma@amc.uva.nl  
(P.J. Bosma)

## Lay summary

Progressive familial intrahepatic cholestasis type 3 (PFIC3) is a severe genetic liver disease that results from impaired transport of lipids to bile, which makes the bile toxic to liver cells. Because therapeutic options are currently limited, this study aims to evaluate gene therapy to correct the underlying genetic defect in a mouse model of this disease. By introducing a functional copy of the missing gene in liver cells of mice, we were able to restore lipid transport to bile and strongly reduce damage to the liver. The proliferation of liver cells was also reduced, which contributes to long-term correction of the phenotype. Further studies are required to evaluate whether this approach can be applied to patients with PFIC3.



# Liver-directed gene therapy results in long-term correction of progressive familial intrahepatic cholestasis type 3 in mice

Sem J. Aronson<sup>1</sup>, Robert S. Bakker<sup>1</sup>, Xiaoxia Shi<sup>1</sup>, Suzanne Duijst<sup>1</sup>, Lysbeth ten Bloemendaal<sup>1</sup>, Dirk R. de Waart<sup>1</sup>, Joanne Verheij<sup>2</sup>, Giuseppe Ronzitti<sup>3</sup>, Ronald P. Oude Elferink<sup>1</sup>, Ulrich Beuers<sup>1</sup>, Coen C. Paulusma<sup>1</sup>, Piter J. Bosma<sup>1,\*</sup>

<sup>1</sup>Amsterdam University Medical Centers, University of Amsterdam, Tytgat Institute for Liver and Intestinal Research, Amsterdam Gastroenterology and Metabolism, Meibergdreef 9, Amsterdam, The Netherlands; <sup>2</sup>Amsterdam University Medical Centers, University of Amsterdam, Department of Pathology, Meibergdreef 9, Amsterdam, The Netherlands; <sup>3</sup>INTEGRARE, Genethon, INSERM, University of Evry, University Paris-Saclay, 91002 Evry, France

**Background & Aims:** Progressive familial intrahepatic cholestasis type 3 (PFIC3), for which there are limited therapeutic options, often leads to end-stage liver disease before adulthood due to impaired ABCB4-dependent phospholipid transport to bile. Using adeno-associated virus serotype 8 (AAV8)-mediated gene therapy, we aimed to restore the phospholipid content in bile to levels that prevent liver damage, thereby enabling stable hepatic ABCB4 expression and long-term correction of the phenotype in a murine model of PFIC3.

**Methods:** Ten-week-old *Abcb4*<sup>-/-</sup> mice received a single dose of AAV8-hABCB4 (n = 10) or AAV8-GFP (n = 7) under control of a liver specific promoter via tail vein injection. Animals were sacrificed either 10 or 26 weeks after vector administration to assess transgene persistence, after being challenged with a 0.1% cholate diet for 2 weeks. Periodic evaluation of plasma cholestatic markers was performed and bile duct cannulation enabled analysis of biliary phospholipids. Liver fibrosis and the Ki67 proliferation index were assessed by immunohistochemistry.

**Results:** Stable transgene expression was achieved in all animals that received AAV8-hABCB4 up to 26 weeks after administration. AAV8-hABCB4 expression restored biliary phospholipid excretion, increasing the phospholipid and cholesterol content in bile to levels that ameliorate liver damage. This resulted in normalization of the plasma cholestatic markers, alkaline phosphatase and bilirubin. In addition, AAV8-hABCB4 prevented progressive liver fibrosis and reduced hepatocyte proliferation for the duration of the study.

**Conclusion:** Liver-directed gene therapy provides stable hepatic ABCB4 expression and long-term correction of the phenotype in a murine model of PFIC3. Translational studies that verify the clinical feasibility of this approach are warranted.

**Lay summary:** Progressive familial intrahepatic cholestasis type 3 (PFIC3) is a severe genetic liver disease that results from impaired transport of lipids to bile, which makes the bile toxic to liver cells. Because therapeutic options are currently limited, this study aims to evaluate gene therapy to correct the underlying genetic defect in a mouse model of this disease. By introducing a functional copy of the missing gene in liver cells of mice, we were able to restore lipid transport to bile and strongly reduce damage to the liver. The proliferation of liver cells was also reduced, which contributes to long-term correction of the phenotype. Further studies are required to evaluate whether this approach can be applied to patients with PFIC3.

© 2019 European Association for the Study of the Liver. Published by Elsevier B.V. This is an open access article under the CC BY-NC-ND license (<http://creativecommons.org/licenses/by-nc-nd/4.0/>).

## Introduction

Progressive familial intrahepatic cholestasis type 3 (PFIC3) is an autosomal-recessive liver disorder. Patients with PFIC3 present with cholestasis at a young age, which progresses to cirrhosis and end-stage liver disease before adulthood.<sup>1–3</sup> PFIC3 is caused by impairment of phosphatidylcholine (PC) translocation to bile by the canalicular membrane protein ATP binding cassette subfamily B member 4 (ABCB4), formerly known as multidrug resistance protein 3 (MDR3), encoded by the *ABCB4* gene.<sup>4–6</sup> In bile, PC is essential in the formation of mixed micelles with bile salts that protect the lining of the biliary tree from the detergent properties of bile salts. In the absence of PC transport, bile salt-induced cytotoxicity causes progressive destruction of cholangiocytes, mainly of small bile ducts, and hepatocytes leading to intrahepatic cholestasis and progressive liver damage.<sup>4,7</sup>

Currently, therapeutic options for PFIC3 are limited. Treatment with ursodeoxycholic acid (UDCA) achieves biochemical improvement by its anticholestatic effects and by stimulating biliary HCO<sub>3</sub><sup>-</sup> secretion at the level of the hepatocyte and cholangiocyte, shielding the cellular membranes from entry of toxic protonated glycine-conjugated bile salts (biliary HCO<sub>3</sub><sup>-</sup> umbrella hypothesis).<sup>3,8,9</sup> Evidence for long-term clinical benefit is lacking due to the lack of prospective randomized, placebo-controlled trials. Partial external biliary diversion (PEBD) is the primary surgical intervention in the management of patients

Keywords: Progressive familial intrahepatic cholestasis; PFIC type 3; PFIC3; ABCB4; MDR3; MDR2; Adeno-associated virus; AAV; AAV8; Gene therapy; Correction cholestatic phenotype.

Received 18 January 2019; received in revised form 1 March 2019; accepted 21 March 2019; available online 29 March 2019

\* Corresponding author. Address: Tytgat Institute for Liver and Intestinal Research, Department of Gastroenterology and Hepatology, Amsterdam UMC, University of Amsterdam, Room S1-168, Meibergdreef 69, 1105 BK Amsterdam, The Netherlands. Tel.: +31 20 566 8850.

E-mail address: [p.j.bosma@amc.uva.nl](mailto:p.j.bosma@amc.uva.nl) (P.J. Bosma).



with PFIC and can postpone the need for eventual liver transplantation, but only if attempted before major liver damage has occurred.<sup>10,11</sup> We have to note that the reported number of PEBD performed in patients with PFIC3, as opposed to those with PFIC1 and PFIC2, is extremely low and that only a marginal therapeutic effect can be expected based on the pathophysiology. Liver transplantation is the only curative treatment for PFIC3. Despite the risk of short- and long-term complications after liver transplantation and procedure-associated mortality, the reported patient survival of 75–100% and primary graft survival of 73–89% are high.<sup>12,13</sup> It is mainly the lifetime burden of immunosuppressive therapy and the limited availability of donor livers that warrant the development of alternative therapeutic strategies.

Adeno-associated virus (AAV) vector mediated gene therapy is an attractive, potentially curative approach to treat inherited gene deficiencies and has taken a leap towards clinical application in the last decade. AAV-mediated transfer of a functional copy of the clotting factor IX gene into hepatocytes has shown to be safe and provided a long-term reduction of bleeding episodes in patients with hemophilia B.<sup>14</sup> This approach is currently under clinical investigation for other indications such as Crigler-Najjar syndrome (NCT03466463),<sup>15</sup> Mucopolysaccharidosis type VI (NCT03173521)<sup>16</sup> and Pompe disease (NCT03533673).<sup>17</sup> The AAV system is established as the vector of choice because of its superior safety profile and non-integrative nature.<sup>18</sup> AAV-mediated gene transfer results in episomal transgene expression, which is a major safety advantage over gene editing approaches, but has limited its application to quiescent tissue to reduce the chance of gradual vector loss upon cell division.<sup>19–21</sup> Low transgene persistence is expected when targeting proliferative tissue. This is especially undesirable since effective vector re-administration is impaired by neutralizing antibody formation, triggered by the initial vector exposure.<sup>22</sup> Despite the current paradigm, we believe that AAV-mediated gene therapy directed to the liver can be an attractive approach to treat PFIC3 even though the disorder is associated with considerable hepatocyte proliferation. For a single dose of AAV vector to be effective and provide long-term correction in PFIC3, it would be necessary to completely eliminate the proliferative trigger and achieve stable transgene expression. Our current study was set up to test this hypothesis.

Expression of only low levels of hepatic ABCB4 results in sufficient phospholipid translocation to bile to prevent liver pathology as shown by studies performed in the *Abcb4*<sup>-/-</sup> mouse, a well characterized model for PFIC3.<sup>7,23,24</sup> Hepatic expression of human *ABCB4* (*hABCB4*) in the *Abcb4*<sup>-/-</sup> mouse at only 15% of wild-type levels improved the phenotype by partly restoring phospholipid content in bile, while in heterozygous animals (*Abcb4*<sup>+/-</sup>) no liver pathology is observed.<sup>25</sup> The phenotype in mice is relatively modest compared to that in humans because of a less toxic bile salt composition in bile, but it can be aggravated by adding the hydrophobic bile salt cholate to the diet to more closely resemble the human PFIC3 phenotype.<sup>26</sup> As a proof-of-concept study we developed a liver-targeting gene therapy strategy to correct the phenotype in a murine model of PFIC3. We hypothesized that AAV-mediated transfer of *hABCB4* to the liver of *Abcb4*<sup>-/-</sup> mice could provide stable transgene expression by restoring biliary phospholipid excretion to levels that eliminate hepatocyte proliferation and result in long-term correction of the phenotype.

Materials and methods

Plasmid design and vector production

The *hABCB4* gene comprises 27 coding exons and spans approximately 78 kb on chromosome 7 (NCBI Gene ID: 5244), resulting in cDNA of 3.8 kb. A transgene expression cassette was assembled by cloning the *hABCB4* cDNA (GenBank: M23234.1) into a modified AAV expression cassette derived from a previously described vector<sup>27</sup> that includes the wild-type AAV2 inverted terminal repeats (ITRs), an apolipoprotein E gene-derived enhancer and a compact liver specific human alpha 1-antitrypsin (*hAAT*) promoter (Fig. 1A). The human factor IX-derived synthetic intron and the bovine growth hormone gene polyadenylation signal were also included to improve mRNA stability.<sup>28</sup> A vector containing green fluorescent protein (GFP) was used as a control, AAV8-GFP. This control vector, containing the *hAAT* promoter, had a similar backbone compared to the experimental vector. AAV vectors were produced using an adenovirus-free transient transfection method as previously described.<sup>15,29</sup> In brief, adherent human embryonic kidney cells (HEK293T) were transfected with AAV2 Rep and AAV8 Cap (pDP8.ape, Plasmid Factory, Bielefeld, Germany) and the ITR-flanked transgene expression cassette. After 72 h of transfection cells were harvested, lysed by 2 freeze–thaw cycles and treated with DNase, RNase (Roche, Basel, Switzerland) and benzonase (Merck, Darmstadt, Germany). Vectors were then purified by iodixanol gradient ultra-centrifugation. Titers of AAV vector stocks were determined using quantitative real-time polymerase chain reaction (qPCR) with primers directed to the promoter sequence as mentioned in Table S1.

Assessment of vector genome integrity and transduction capacity in vitro

Taking the maximal AAV packaging capacity of ~5 kb into account, we assessed if the AAV8-*hABCB4* vector genome

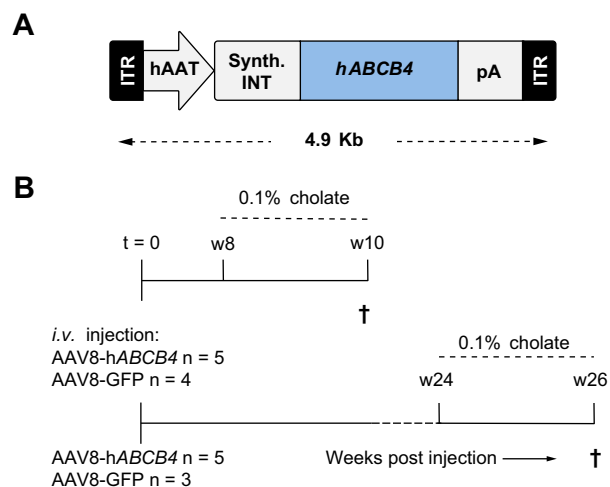


**Fig. 1. Schematic representation of vector expression cassette and experimental design.** (A) Schematic representation of the AAV8-*hABCB4* vector genome consisting of an expression cassette including a liver specific *hAAT* promoter, a factor IX-derived synthetic intron (Synth. INT), the *hABCB4* coding sequence and a polyadenylation signal (pA), flanked by AAV2 ITRs. (B) At t = 0, 10-week-old male *Abcb4*<sup>-/-</sup> mice received intravenous administration of AAV8-*hABCB4* (n = 10) or AAV8-GFP control (n = 7) at a dose of 5 × 10<sup>13</sup> vg/kg. All animals were challenged by a 0.1% cholate diet for a duration of 2 weeks, starting either at 8 or 24 weeks after vector administration. AAV, adeno-associated virus; GFP, green fluorescent protein; *hABCB4*, human *ABCB4*; *hAAT*, human alpha 1-antitrypsin; ITRs, inverted terminal repeats.

(4.9 kb) was completely packaged using Southern blot analysis. DNA was extracted from  $1 \times 10^8$  vector particles by heat-denaturation at 96 °C for 5 min and separated by alkaline agarose gel electrophoreses. Digoxigenin-dUTP labeled probes directed to the promoter sequence were produced using a PCR digoxigenin Probe Synthesis Kit (Merck, Darmstadt, Germany) and used for DNA hybridization as described previously.<sup>30</sup> Transduction of a human hepatoma cell line (Huh7) with the AAV8-hABC $B_4$  vector at  $5 \times 10^6$  gc/cell was performed in a 6-well plate in 1 ml Dulbecco's modified Eagle's medium (DMEM; Lonza, Cologne, Germany) supplemented with 4 mmol/L L-glutamine and a mixture of antibiotics (5 mg/ml penicillin, 5 mg/ml streptomycin). After 4 h, 1 ml of complete DMEM (containing 10% foetal calf serum) was added and incubated for 72 h before cells were lysed and expression of ABC $B_4$  was confirmed by western blot using the monoclonal antibody P $_3$ II-26 (Merck, Darmstadt, Germany) as previously described.<sup>31</sup> To achieve higher transduction efficiency *in vitro* the Huh7 cells were pre-treated for 2 h with 1  $\mu$ M etoposide to enhance the DNA damage response, which increases second-strand synthesis by inhibition of topoisomerase II.<sup>32,33</sup>

### Animal study procedures

Ten-week-old male *Abcb4* knockout mice (C57BL/6 background) randomly received a single administration of either AAV8-hABC $B_4$  (n = 10) or AAV8-GFP control (n = 7) at a dose of  $5 \times 10^{13}$  vector genome copies per kg via tail vein injection. Mice were housed in a temperature-controlled environment with 12 h/12 h light–dark cycle and permitted *ad libitum* consumption of standard chow (2016 Teklad global 16% protein rodent diet, Envigo, Huntingdon, United Kingdom) and water. All animals were challenged with 0.1% cholate supplemented to the standard chow for a duration of 2 weeks until termination, starting either at 8 or 24 weeks after vector administration (Fig. 1B). Blood sampling was performed every 2 weeks and every week during dietary challenge. Prior to termination, bile duct cannulation was performed under anesthesia with ketamine (Nimatek, 100 mg/kg) and xylazine (Sedamun, 10 mg/kg) as previously described.<sup>34</sup> Bile was collected in aliquots every 10 min for 30 min after distal ligation of the common bile duct. Bile flow was determined gravimetrically assuming a density of 1 g/ml for bile. Additionally, bile was collected directly from the gallbladder by a 30 G needle prior to bile duct cannulation. Blood was collected by cardiac puncture and plasma was separated by centrifugation at 1,000 g for 5 min. Organs were fixed overnight in 4% paraformaldehyde or snap frozen in liquid N $_2$  and stored at –80 °C for further analysis. All animal experiments were performed in accordance with the European Directive 2010/63/EU and with approval of the Institutional Animal Care and Use Committee of the Amsterdam UMC.

### Biochemistry and bile analysis

Plasma biochemistry for cholestatic markers (alkaline phosphatase [ALP], total bilirubin) and liver injury (alanine aminotransferase [ALT], aspartate aminotransferase [AST]) were determined by routine clinical biochemistry testing on a Roche Cobas c502/702 analyzer (Roche Diagnostics, US). Choline containing phospholipids and cholesterol in bile were determined enzymatically as described previously.<sup>35</sup> Determination of changes in fluorescence were performed on a CLARIOstar analyzer (BMG Labtech, Offenburg, Germany). Concentrations of different bile salt species in plasma and bile were determined

by reverse-phase high-performance liquid chromatography as described previously.<sup>36</sup>

### Transgene expression

Genomic DNA was isolated as previously described<sup>37</sup> from at least 8 random pieces from 4 different lobes to minimize sampling error. hABC $B_4$  and GFP copy number were determined by qPCR in a LightCycler480 (Roche Diagnostics USA) using the SensiFAST™ SYBR No-ROX kit (GC Biotech, Waddinxveen, the Netherlands) and the primers mentioned in Table S1. Results were processed and analyzed using LinRegPCR software and normalized to the geometric mean of *36b4* and *Gapdh*. To determine the expression of both the hABC $B_4$  and GFP genes, total liver RNA was isolated as previously described using Trizol,<sup>37</sup> according to the same method to minimize sampling error. Two micrograms of RNA were then reverse transcribed to cDNA using the RevertAid cDNA Synthesis Kit (Thermo Scientific) with random hexamers and oligo dT primers. qPCR was performed on a LightCycler480 (Roche Diagnostics, Indianapolis, USA) using SensiFAST™ SYBR No-ROX kit (GC Biotech, Waddinxveen, the Netherlands) and the primers mentioned in Table S1. Results were normalized to the geometric mean of *36b4*, *Gapdh* and *Hprt*. Determination of both genomic DNA and RNA in the liver was performed twice after a second, independent DNA and RNA isolation.

### Anti-hABC $B_4$ antibody assay

Antibody detection was performed using an ELISA assay as previously described.<sup>38</sup> Lysates of Madin-Darby Canine Kidney (MDCK) cells or MDCK cells overexpressing hABC $B_4$  were used to coat ELISA plates (Greiner, Kremsmünster, Austria) overnight with 2  $\mu$ g protein per well in 50 mM carbonate buffer pH 9.6. The wells were blocked with 1% gelatin in PBS, washed and incubated with serial dilutions of mouse plasma. After washing, mouse immunoglobulins were detected with peroxidase conjugated goat-anti-mouse IgG followed by o-phenylenediamine (Merck, Darmstadt, Germany) conversion. For the determination of anti-hABC $B_4$  antibody titers, the titer of the same sample on the negative control plate (MDCK lysate coated) was subtracted to correct for non-specific binding.

### Histology

For conventional bright-field light microscopy, livers were fixed in 4% formaldehyde solution and embedded in paraffin. Five-micron sections were stained with hematoxylin (Sigma, 51275) and Eosin (Sigma, E4382) (H&E) or Sirius red.<sup>39</sup> Semi-quantitative analysis of liver fibrosis<sup>40</sup> was performed by a senior hepatopathologist (JV) blinded to the experimental groups. By using the following scoring system, ranging from 0 to 4, we were able to assess features such as distribution and fibrous bridging: 0 no fibrosis, 1 periportal fibrosis in <50% of portal fields; 2 periportal fibrosis in >50% of portal fields; 3 bridging fibrosis in <50% of portal fields; 4 bridging fibrosis in >50% of portal fields. Acute liver injury in the *Abcb4*<sup>-/-</sup> model was assessed by monitoring ALT and AST.

### Immunohistochemistry

For the detection of hABC $B_4$ , cryosections (5  $\mu$ m) were fixed in acetone and stained with the monoclonal antibody P $_3$ II26 (Enzo Life Sciences, Farmingdale, NY, USA) as previously described.<sup>41</sup> For the detection of GFP (anti-GFP, Rockland) and Ki67 (SP6, Thermo Scientific) the same procedure was performed. In short,

endogenous peroxidase was blocked by incubating slides with 0.3% H<sub>2</sub>O<sub>2</sub> in PBS for 15 min. Slides were incubated with the primary antibody (1:2,000) for 4 h at room temperature, rinsed and incubated with secondary antibody horse radish peroxidase (HRP) G-anti-Ms/Rb IgG (DPVB110HRP Immunologic) for 45 min. Subsequently the slides were incubated with Bright DAB substrate (BS04-110, ImmunoLogic) for 7 min. Counterstaining was performed with hematoxylin. Ki67-positive hepatocyte nuclei were manually counted by 2 observers (LtB and SA) in 5 randomly-selected, non-overlapping microscopic fields at 20× magnification. For the detection of cytokeratin 7 (CK7) (EPR17078, Abcam) the above procedure was performed except that the endogenous peroxidase was blocked by incubating slides with 0.3% H<sub>2</sub>O<sub>2</sub> in methanol and the secondary antibody was visualized using the NovaRED™ Peroxidase (HRP) Substrate Kit (Vector Laboratories, Burlingame, CA, USA).

**RNA in situ hybridization**

For the detection of target RNA in liver tissue we made use of the RNAscope® technology according to the manufacturer’s protocol (Advanced Cell Diagnostics, Inc., Hayward, CA, USA). Target probes for hABC4 and GFP based on the sequences mentioned in Table S1 were hybridized on liver tissue and visualized after signal amplification with fast-red, and counterstained using hematoxylin. UBC and dapB probes served as positive and negative controls, respectively.

**Statistical analysis**

Data are presented as mean values ± SD and were analyzed for significance using the independent 2-tailed *t* test for the comparison of parametric variables between 2 groups, unless stated otherwise. For non-parametric variables we performed a Mann-Whitney *U* test and for the comparison of 3 or more groups a 1-way analysis of variance (ANOVA) was performed. To assess the inter-observer agreement for the quantification of the Ki67 proliferation index the correlation coefficient was calculated between the analysis of the 2 observers. For statistical analysis we used GraphPad Prism 7 software (GraphPad Software Inc., CA, USA). \**p* < 0.05, \*\**p* < 0.01, \*\*\**p* < 0.001 were considered significant.

For further details regarding the materials and methods used, please refer to the [Supplementary CTAT table](#).

**Results**

**Design and in vitro validation of a viral vector for the treatment of PFIC3**

The AAV8-hABC4 vector genome is relatively large (4.9 kb) and approaches the maximal AAV packaging capacity of ~5 kb. The expression cassette includes the hABC4 cDNA with a length of 3.8 kb under control of a liver specific hAAT promoter (Fig. 1A). Vector genome integrity was evaluated by Southern blot analysis of the heat-denatured AAV8-hABC4 vector, showing both

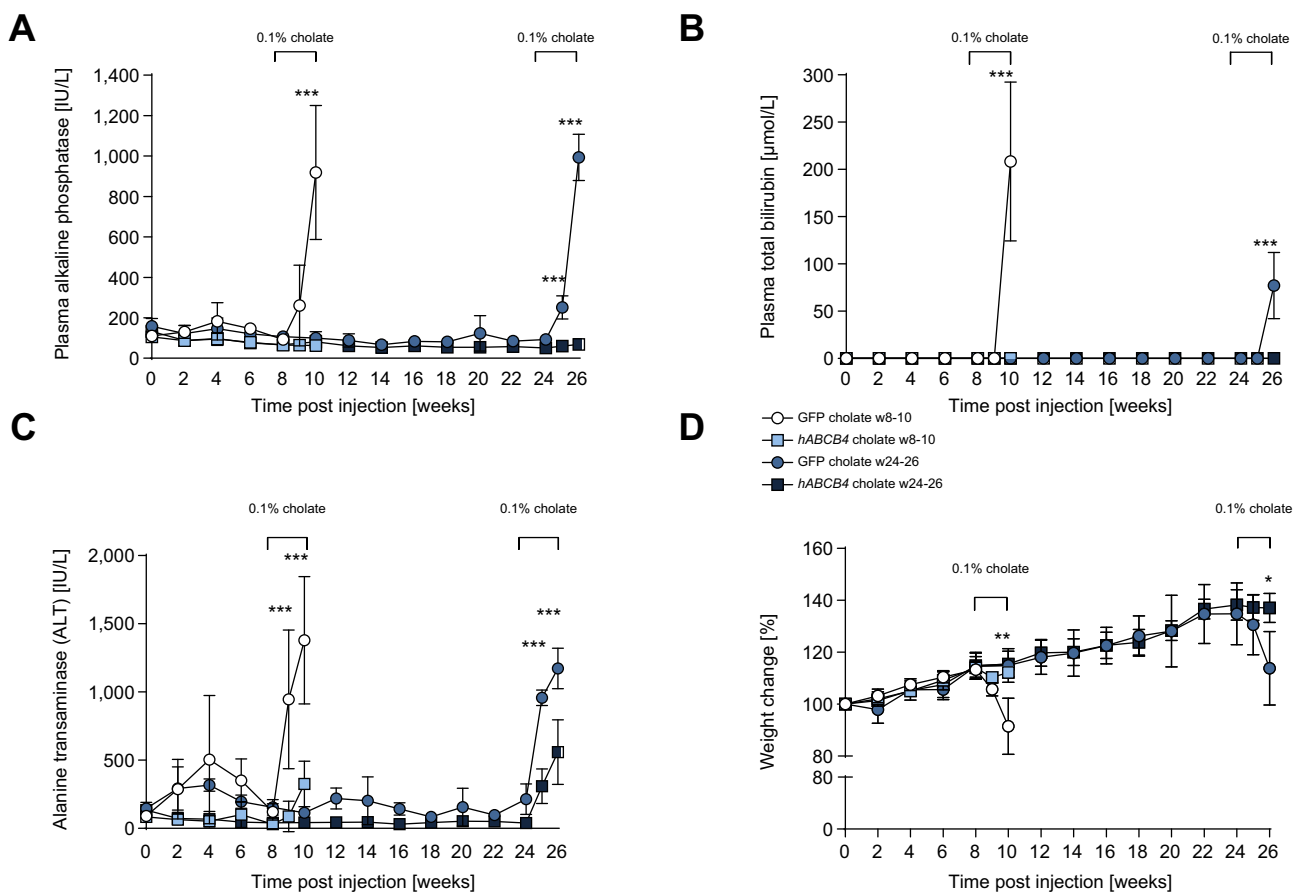


**Fig. 2. AAV8-hABC4 corrects the cholestatic phenotype in *Abcb4*<sup>-/-</sup> mice.** (A-C) Plasma biochemistry shows cholestatic markers (ALP in IU/L and total bilirubin in µmol/L) and parenchymal liver injury (ALT in IU/L) of animals treated with AAV8-hABC4 (light blue; n = 5 and black; n = 5) or AAV8-GFP (white; n = 4 and dark blue; n = 3). The time during which animals are challenged with a 0.1% cholate diet is indicated. (D) Body weight change of mice over time is represented as the mean ± SD at separate time points for all 4 groups. \**p* < 0.05, \*\**p* < 0.01, \*\*\**p* < 0.001 by independent 2-tailed *t* test. AAV, adeno-associated virus; ALP, alkaline phosphatase; ALT, alanine aminotransferase; GFP, green fluorescent protein; hABC4, human ABCB4.

full-length and partial genomes (Fig. S1A). Transduction of Huh7 cells with the AAV8-hABC*B4* vector resulted in expression of ABC*B4*, confirmed by western blot (Fig. S1B).

**AAV8-hABC*B4* corrects the cholestatic phenotype in *Abcb4*<sup>-/-</sup> mice**

Ten-week-old male *Abcb4*<sup>-/-</sup> mice received a single administration of AAV8-hABC*B4* (n = 10) or AAV8-GFP control (n = 7) at a dose of 5 × 10<sup>13</sup> vector genome copies per kg via tail vein injection. All animals were challenged by a 0.1% cholate diet for a duration of 2 weeks before termination, starting either at 8 or 24 weeks after vector administration (Fig. 1B). This dietary challenge led to a steep increase of the cholestatic markers ALP and total bilirubin in plasma of animals that received the AAV8-GFP control vector (Fig. 2A and B), as expected in the *Abcb4*<sup>-/-</sup> model.<sup>26</sup> In contrast, treatment with the AAV8-hABC*B4* vector resulted in complete correction of this cholestatic phenotype, both at the early (w8-10) and the late (w24-26) time point (Fig. 2A and B). Serum ALT, an indicator of parenchymal liver damage, was also markedly reduced in animals treated with AAV8-hABC*B4* compared to controls during cholate feeding (Fig. 2C). High levels of total bile salts were measured in plasma of AAV8-GFP treated animals after 2 weeks of cholate diet, which were markedly lower in plasma of AAV8-hABC*B4* treated animals (1.94 ± 0.54 vs. 0.013 ± 0.006 mM, p < 0.001). The con-

centrations of total bile salts in plasma, of which >90% was conjugated cholate, are presented in Table S2. The severe cholestasis and increase in serum aminotransferases in animals treated with the control vector translated to significant weight loss (-21.8% week 10 vs. week 8; -20.9% week 26 vs. week 24), while the weight of animals treated with AAV8-hABC*B4* remained stable (Fig. 2D). After termination, both the normalization of relative liver weight and the strong reductions in gallbladder volume (135 ± 28 μl [n = 7] vs. 5 ± 2 μl [n = 10], p < 0.001) indicated a marked effect of the vector in AAV8-hABC*B4* treated mice (Fig. S2).

**AAV8-hABC*B4* restores phospholipid and cholesterol content in bile**

At the end of the experiments, bile collection enabled determination of biliary phospholipid and cholesterol content. In animals treated with AAV8-hABC*B4* the phospholipid and cholesterol content in bile was restored to levels that were comparable to levels reported in *Abcb4*<sup>+/+</sup> mice<sup>7</sup> (Fig. 3A-B). The restoration of phospholipid and cholesterol content in bile was persistent up to 26 weeks after vector administration. Bile flow was assessed in all animals that were successfully cannulated, and no differences were seen between the groups (Fig. 3C). Phospholipid output in bile was increased in all animals treated with AAV8-hABC*B4* compared to controls

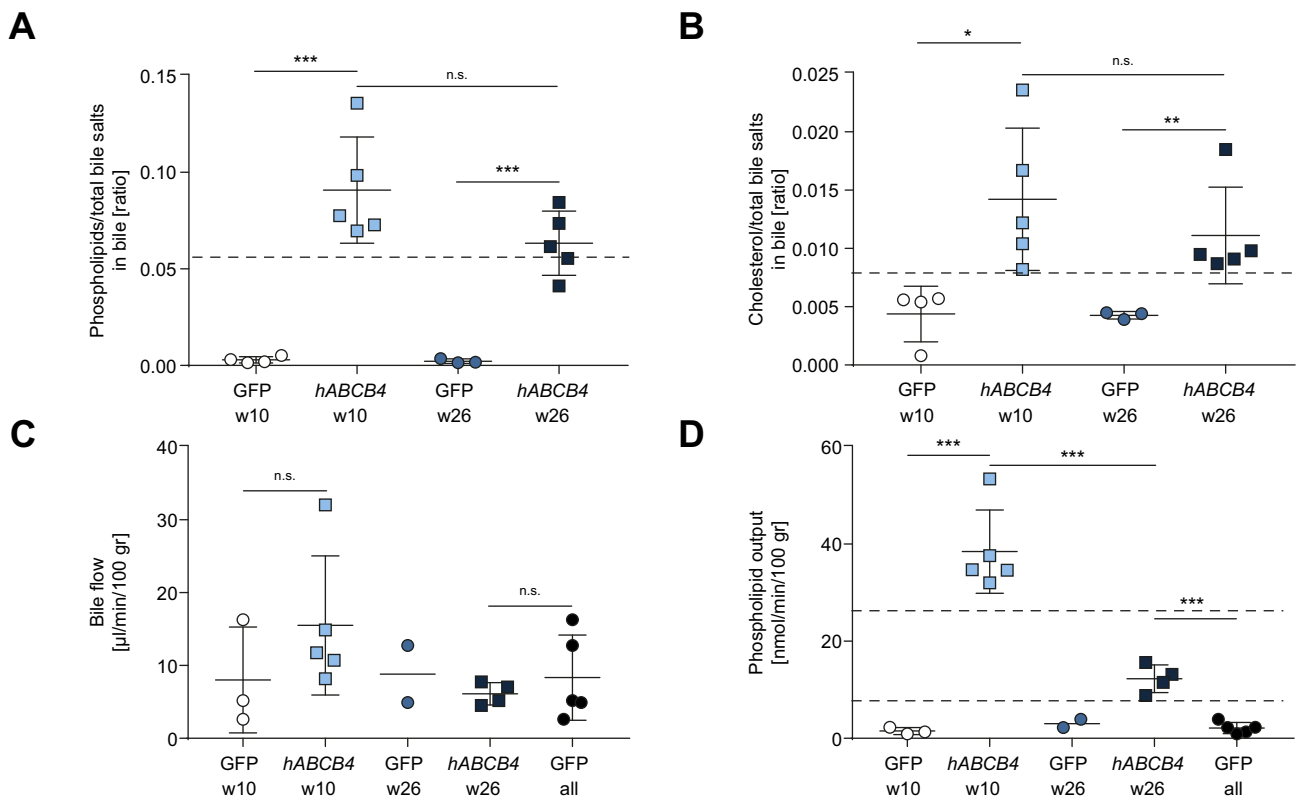


**Fig. 3. AAV8-hABC*B4* restores phospholipid and cholesterol content in bile of *Abcb4*<sup>-/-</sup> mice.** Bile was collected as described in the methods section. Data is presented as mean ± SD for biliary (A) phospholipid and (B) cholesterol content in animals treated with AAV8-hABC*B4* (w10 light blue; n = 5 and w26 black; n = 5) or AAV8-GFP (w10 white; n = 4 and w26 dark blue; n = 3). (C-D) Bile flow and phospholipid output after successful bile cannulation in 14/17 animals treated with AAV8-hABC*B4* (w10 light blue; n = 5 and w26 black; n = 4) or AAV8-GFP (w10 white; n = 3 and w26 dark blue; n = 2). A fifth group consisting of the pooled results from all AAV8-GFP treated animals (black n = 5) was added to compare AAV8-hABC*B4* vs. AAV8-GFP treated animals at time point w26. The mean phospholipid and cholesterol levels in bile of *Abcb4*<sup>+/+</sup> mice<sup>7</sup> (black dotted line) and the threshold of phospholipid output necessary to improve liver damage in mice<sup>25</sup> (lower dotted line) are indicated. n.s. is not significant, \*p < 0.05, \*\*p < 0.01, \*\*\*p < 0.001 by independent 2-tailed t test. AAV, adeno-associated virus; GFP, green fluorescent protein; hABC*B4*, human ABC*B4*.

(Fig. 3D). Although animals at both the early (w8–10) and late (w24–26) time point showed a phospholipid output that was above the threshold required to improve liver damage as described in the literature (15% of wild-type),<sup>25</sup> a relative decrease over time was observed. The absolute concentrations of phospholipids, cholesterol and total bile salts in bile are presented in Table S2.

**AAV8-hABCb4 mediated expression of hABCb4 in liver is stable**

Both hABCb4 transgene copy numbers and mRNA expression were detectable in livers of all animals treated with AAV8-hABCb4 and remained stable for at least 26 weeks, while hepatic GFP transgene and expression in animals treated with AAV8-GFP decreased over time (Fig. 4). Furthermore, hABCb4 expression in the liver remained stable for the duration of the study (26 weeks) (Fig. 5A-B), while GFP expression was reduced when comparing the late (w24–26) to the early (w8-10) time point (Fig. 5C-D). Using *in situ* hybridization with RNA specific probes (RNA scope) we were able to visualize hABCb4 mRNA expression in liver tissue on the cellular level. Immunostaining was used to visualize both hABCb4 and GFP protein expression, showing a clear canalicular staining pattern for hABCb4 and cytosolic expression of GFP (Fig. 6). Since transgene expression was stable for the duration of the experiment but a relative decrease of phospholipid output in bile was observed, we studied the possibility of inactivating anti-ABCb4 antibody formation after vector administration. No ABCb4 antibodies in plasma were detected as a consequence of hABCb4 expression in *Abcb4*<sup>-/-</sup> mice at 26 weeks after vector administration (Fig. S3).

**AAV8-hABCb4 prevents liver fibrosis and reduces hepatocyte proliferation**

Histological evaluation of the liver by hematoxylin and eosin (H&E) staining showed almost complete amelioration of the ductular reaction in AAV8-hABCb4 treated animals compared to AAV8-GFP treated animals, both 10 and 26 weeks after AAV-hABCb4 administration (Fig. 7A). This was subsequently confirmed by immunostaining of cytokeratin-7 in liver sections (Fig. S4). Sirius red staining enabled scoring of fibrosis in the liver, as described in the methods section, and showed a decreased fibrosis score in AAV8-hABCb4 treated animals compared to AAV8-GFP treated animals (Fig. 7A-B). The Ki67 proliferation index tended to decrease after 10 weeks and decreased after 26 weeks in animals that received the AAV8-hABCb4 vector compared to animals that received AAV8-GFP (Fig. 7C-D). Additionally, we assessed the number of Ki67 positive hepatocytes at baseline in untreated *Abcb4*<sup>-/-</sup> mice at 10 weeks of age (Fig. 7D and Fig. S5). Accurate identification of Ki67-positive hepatocytes is known to be difficult.<sup>42</sup> Still, the correlation coefficient between the analyses of the 2 observers was R<sup>2</sup> 0.87 (*p* < 0.001). No macroscopic or microscopic signs of liver tumors were found in any of the animals during the experimental period. Spontaneous development of liver tumors has been described in the *Abcb4*<sup>-/-</sup> mouse, but is strongly dependent on the genetic background of the strain<sup>23,26</sup> and has not previously been described before the age of 12 months in the C57BL/6 strain.

**Discussion**

PFIC3 is a severe, inherited liver disorder caused by hepatic ABCb4 deficiency. Impaired phospholipid excretion into bile

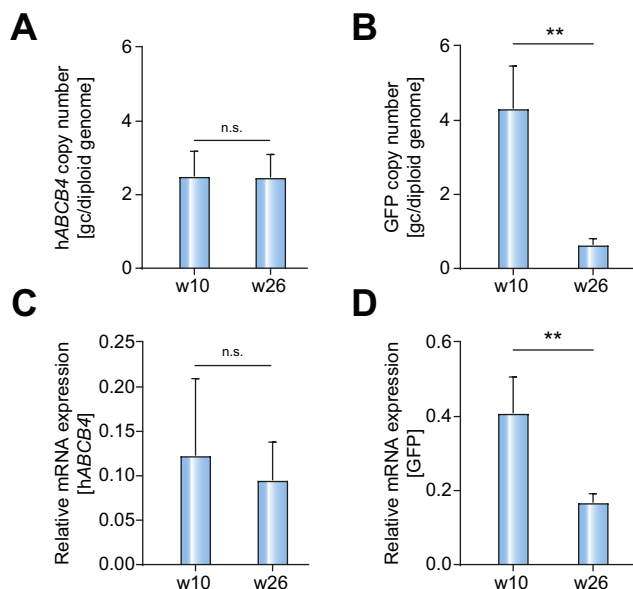


**Fig. 4. AAV8-hABCb4 mediated expression of hABCb4 in liver is stable, while GFP expression is lost over time.** Transgene copy number of (A) hABCb4 and (B) GFP and relative mRNA expression of (C) hABCb4 and (D) GFP in liver of animals treated with AAV8-hABCb4 (w10; n = 5 and w26; n = 5) or AAV8-GFP (w10; n = 4 and w26; n = 3). Expression of hABCb4 was undetectable in AAV8-GFP treated animals and expression of GFP was undetectable in AAV8-hABCb4 treated animals. Experiment is performed in duplicate with separate RNA and DNA isolation, data is presented as mean ± SD. n.s. is not significant, \*\**p* < 0.01. AAV by independent 2-tailed *t* test, adeno-associated virus; GFP, green fluorescent protein; hABCb4, human ABCb4.

leads to bile salt-induced damage to bile duct epithelial cells and hepatocytes, resulting in cholestasis and progressive fibrosis. Currently, therapeutic options for PFIC3 are limited and in the majority of cases a liver transplantation is inevitable. We aimed to develop AAV-mediated, liver-directed gene therapy to correct the ABCb4 deficiency, restore phospholipid excretion into bile and prevent liver injury. Liver-directed gene therapy using AAV vectors has proven to be safe and effective for the treatment of hemophilia B<sup>14</sup> and has great potential for the treatment of other inherited disorders as long as the liver tissue itself is not hyperproliferative.<sup>15-17</sup> It is well established that AAV-mediated gene transfer results in stable correction of quiescent tissue and that cell proliferation results in loss of the episomal transgene.<sup>19-21</sup> This fuels the paradigm that AAV-mediated gene therapy in disorders that result in liver damage and subsequent hyperproliferation, such as PFIC3, can only lead to transient correction. Since re-administration of the vector is impaired by anti-AAV neutralizing antibody formation, a transient correction means that an AAV approach will not be curative. However, here we show pre-clinical data suggesting that a single dose of AAV8-hABCb4 in the *Abcb4*<sup>-/-</sup> mouse results in stable hepatic expression of hABCb4 and provides long lasting correction of the phenotype.

In this study, hepatic expression of hABCb4 is achieved up to 26 weeks after vector administration, restoring biliary phospholipid excretion to levels that prevent liver damage and normalize plasma cholestatic markers. The amount of hepatic ABCb4 reconstitution that is necessary to correct the phospholipid content in bile and prevent liver injury in *Abcb4*<sup>-/-</sup> mice is estimated to be between 15–50%.<sup>25,41</sup> In animals that received AAV8-hABCb4, biliary phospholipid and cholesterol content

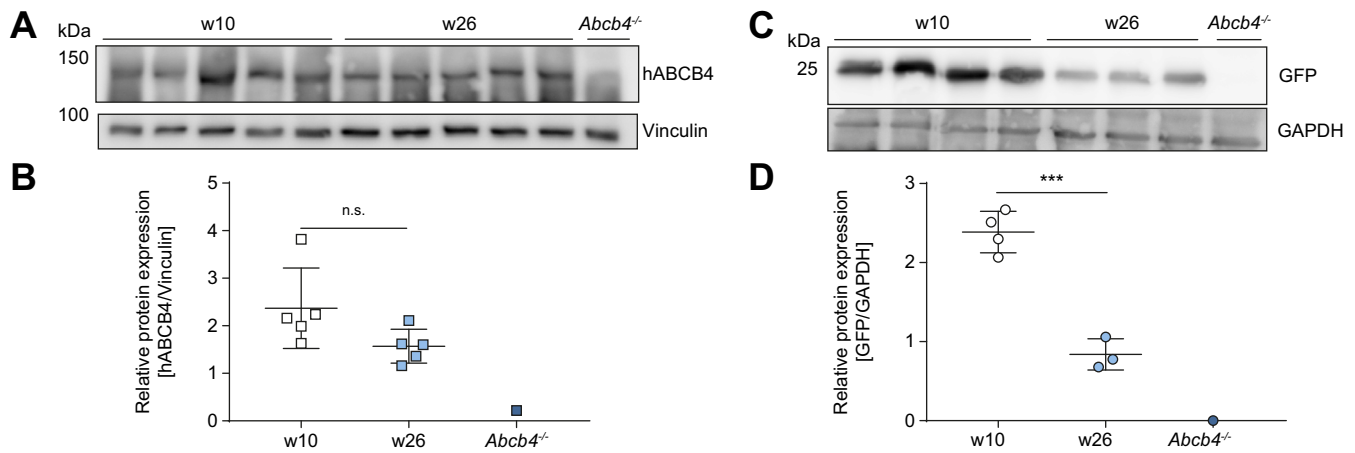


**Fig. 5. ABCB4 protein expression in liver is stable while expression of GFP decreases over time.** Hepatic expression of (A-B) hABCb4 in animals treated with AAV8-hABCb4 (w10; n = 5 and w26; n = 5) and (C-D) GFP in animals treated with AAV8-GFP (w10; n = 4 and w26; n = 3) was confirmed by western blot. Liver lysate of *Abcb4*<sup>-/-</sup> serves as negative control (black; n = 1). n.s. is not significant, \*\*\*p < 0.001. AAV, adeno-associated virus; GFP, green fluorescent protein; hABCb4, human ABCB4.

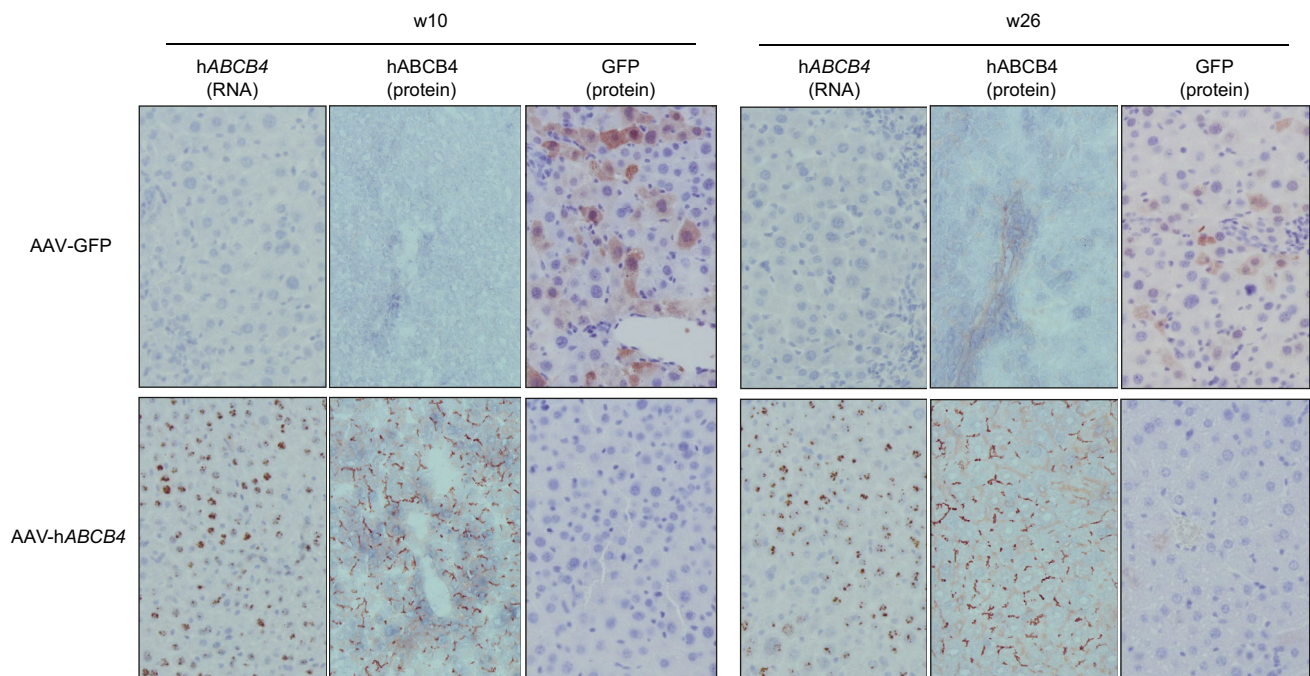


**Fig. 6. Transgene expression on RNA and protein level in liver of AAV8-hABCb4 and AAV8-GFP treated animals.** Representative images (20×) of transgene expression in liver tissue of animals that received a single injection of the indicated vector and were sacrificed at the indicated time point after 2 weeks of 0.1% cholate diet. *In situ* hybridization with RNA specific probes (RNA Scope) visualizes hABCb4 mRNA expression as brown nuclear staining (left panels). Immunostaining of hABCb4 shows a canalicular staining pattern (middle panels) while GFP shows a cytosolic staining pattern (right panels). AAV, adeno-associated virus; GFP, green fluorescent protein; hABCb4, human ABCB4. (This figure appears in colour on the web.)

was restored to wild-type levels and both RNA and protein were detected in 60–80% of hepatocytes, suggesting that hepatic ABCB4 expression levels above 50% of wild-type were reached (Figs. 3 and 6, respectively). The restoration of ABCB4 expression and function resulted in complete correction of the cholestatic phenotype (Fig. 2). We also observed a normalization of the gallbladder size in animals treated with AAV8-hABCb4 (Fig. S2), which could be an indirect effect of resolving the cholestasis in these animals. An increased gallbladder volume has been described previously in *Abcb4*<sup>-/-</sup> mice,<sup>43</sup> but the cause of this phenomenon has not yet been elucidated. We speculate

that the increased gallbladder volume in the AAV-GFP treated mice is the result of severe cholestasis during cholate feeding. Recent studies show that an elevation of plasma bile salts in mice can activate enterocytes to release Fgf15 into the systemic circulation.<sup>36</sup> Elevated systemic Fgf15 levels could result in the increased gallbladder volume, since Fgf15 is known to stimulate gallbladder filling.<sup>44</sup> Besides the correction of the cholestatic phenotype, restoration of ABCB4 function strongly reduces liver fibrosis and dampens hepatocyte proliferation (Figs. 2 and 7, respectively). Both the liver fibrosis score and hepatocyte proliferation are not completely normalized in AAV8-hABCb4 treated

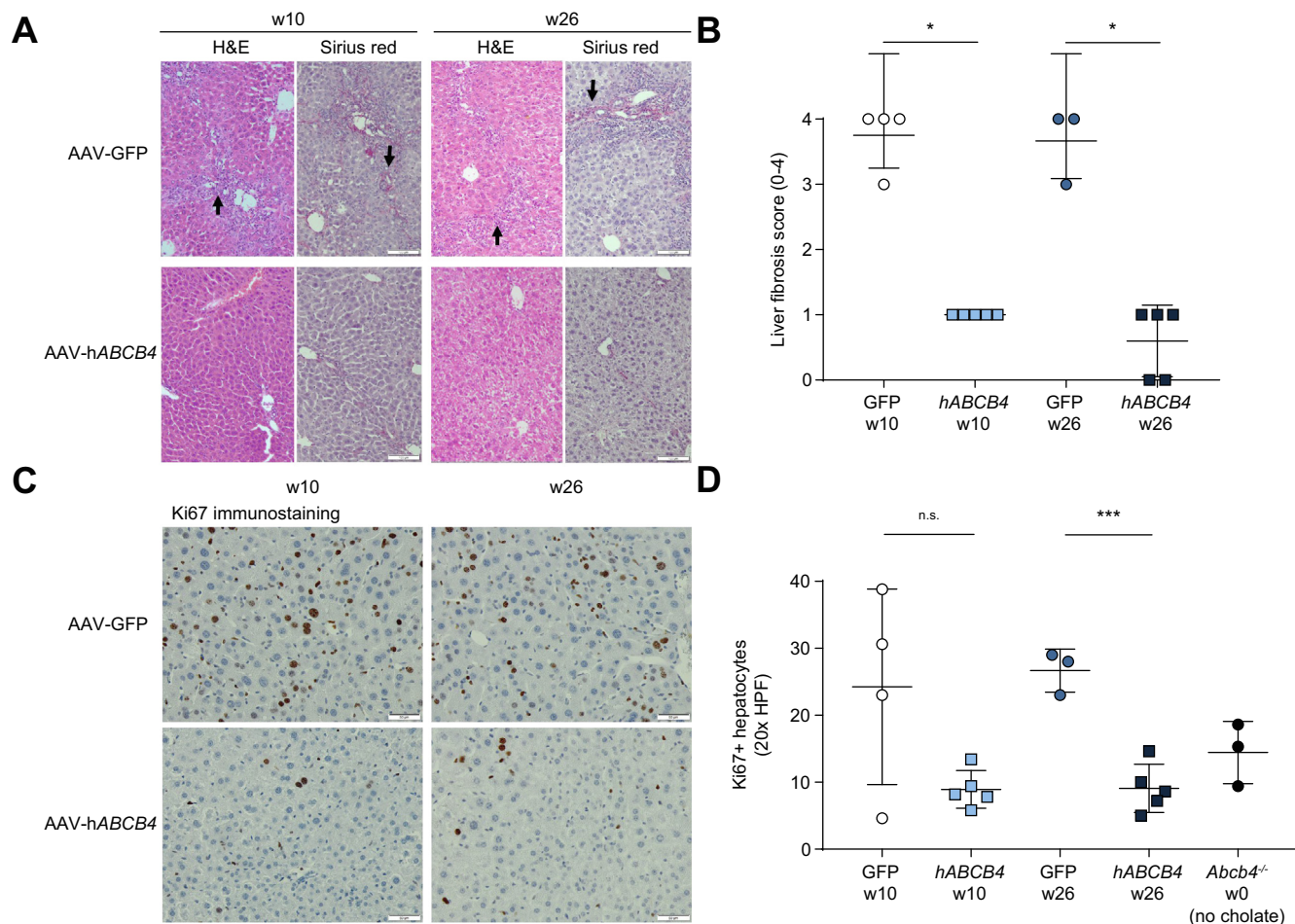


**Fig. 7. AAV8-hABCb4 prevents liver fibrosis and reduces hepatocyte proliferation.** Liver histology in samples of animals that received a single injection of the indicated vector and were sacrificed at the indicated time point after 2 weeks of 0.1% cholate diet. (A) Representative microscopic images (10×) of H&E showing periportal inflammation [↑, arrow upward] and Sirius red staining showing bridging fibrosis [↓, arrow downward] with (B) a quantification of the fibrosis score (see material and methods for details about the quantification). (C) Representative microscopic images (20×) of Ki67 staining with (D) a quantification of Ki67 positive hepatocytes per high power field (20× HPF). An additional group of 10-week-old *Abcb4*<sup>-/-</sup> mice (w0; n = 3) shows the amount of Ki67 positive hepatocytes at baseline. A Mann-Whitney *U* test was used to assess significance for the nonparametric Fibrosis score. n.s. is not significant, \**p* <0.05, \*\**p* <0.01, \*\*\**p* <0.001. AAV, adeno-associated virus; GFP, green fluorescent protein; hABCb4, human ABCb4; H&E, hematoxylin and eosin. (This figure appears in colour on the web.)

animals, but the significant reduction of liver damage is likely to contribute to the long-term transgene expression up to 26 weeks after administration of the vector. Without sufficient correction of the ABCb4 deficiency, constant hepatocyte proliferation would lead to rapid loss of the episomal transgene, as shown in the animals that received AAV8-GFP (Figs. 4 and 5). The level of ABCb4 expression required to prevent liver injury in humans is not known. Even individuals that are heterozygotes for complete loss of function alleles, expressing 50% of hepatic ABCb4, can in some cases develop slowly progressive liver damage.<sup>3,45</sup> Nevertheless, in such cases liver pathology is much less severe and it is safe to assume that in patients with PFIC3, reconstitution of hepatic ABCb4 between 15–50% will probably significantly improve the phenotype and result in a clinically relevant effect.

The *Abcb4*<sup>-/-</sup> mouse model we used in the present study resembles the PFIC phenotype in humans, but some challenges that arise from the difference between the murine model and the human context should be addressed prior to translation of these results. Firstly, the vector was introduced in a liver with relatively modest injury and hepatocyte proliferation. The phe-

notype that spontaneously occurs in AAV-GFP treated animals is limited to flairs of serum ALT (Fig. 2C) and a marginal increase in proliferation of hepatocytes at baseline in 2/3 animals (Fig. 7D). The bile salt composition in mice is less toxic in the absence of phospholipids, leading to a less progressive phenotype than in humans. Young adult *Abcb4*<sup>-/-</sup> mice (~10 weeks old) show modest elevations in serum cholestatic parameters (total bilirubin 9.8 ± 8.0 μmol/L and ALP 173 ± 31 IU/L), serum aminotransferases (ALT 222 ± 80 IU/L) and, histologically, only moderate fibrosis.<sup>7,23</sup> This modest liver injury in young adult mice would resemble a very early disease stage of PFIC3 in humans. Although AAV vector transduction efficacy is probably not limited by liver fibrosis or cirrhosis,<sup>46</sup> the extent of liver injury and subsequent hepatocyte proliferation could be a major factor contributing to gradual loss of transgene expression in humans.<sup>47</sup> To more closely resemble the human phenotype, all animals were challenged with a 0.1% cholate diet as previously described.<sup>26</sup> This diet was introduced either at 8 or 24 weeks after vector administration to assess transgene persistence over time (Fig. 1). Future studies to assess the effect of severe liver injury and abundant hepatocyte proliferation on

AAV-mediated transduction efficacy in the *Abcb4*<sup>-/-</sup> mouse model could be performed by administering AAV8-h*ABCB4* after introducing the cholate diet. Another attractive approach would be to use a mouse model with a humanized bile salt pool that develops a phenotype resembling PFIC3 in humans without a dietary intervention. An example of such a model would be an *Abcb4*<sup>-/-</sup>*Cyp2C70*<sup>-/-</sup> double knockout, which is unable to form hydroxylated bile salts such as  $\alpha$ - or  $\beta$ -muricholate,<sup>48</sup> but this model is currently unavailable.

Secondly, we show efficacy of AAV8-h*ABCB4* in adult *Abcb4*<sup>-/-</sup> mice while PFIC3 in humans presents at young age and most often progresses to end-stage liver disease before adulthood. Ideally, gene therapy should be offered to patients in an early disease stage at young age, but it has been established in prior animal studies that transgene persistence is low in a growing liver.<sup>21</sup> Ongoing experiments of AAV-mediated gene transfer in juvenile *Abcb4*<sup>-/-</sup> mice will give insight into transgene persistence in the context of a growing liver and the minimum hepatic h*ABCB4* expression required to correct the phenotype. Only recently a successful strategy to perform AAV re-administration after impairment of neutralizing antibody formation was described in a pre-clinical setting.<sup>49</sup> Developing strategies that enable retreatment of patients, in whom the therapeutic correction has been lost because of liver growth or residual hepatocyte proliferation, would increase the feasibility of AAV-mediated gene therapy for PFIC3. Furthermore, we acknowledge that an AAV-mediated gene therapy approach could be complementary to existing therapeutic options for PFIC3. Optimal management with UDCA in combination with AAV-mediated gene therapy may contribute to amelioration of liver injury and proliferation, which could achieve the same long-lasting transgene expression seen in the *Abcb4*<sup>-/-</sup> mouse model. Undergoing a liver transplantation will remain the final resort for patients when AAV (re-)administration ceases to confer phenotypic correction. In some cases, AAV8-mediated gene therapy may even become a successful bridging strategy to prevent a liver transplantation at young age.

In conclusion, AAV8-mediated gene therapy provides long-term correction in a murine model of PFIC3, encouraging translational studies that aim to verify AAV-mediated gene therapy as a future option in the management of patients with PFIC3.

### Financial support

This project has received Funding from Metakids to PB [2015-056].

### Conflict of interest

None of the authors have any conflicts of financial interest to disclose, other than mentioned in the financial support statement.

Please refer to the accompanying ICMJE disclosure forms for further details.

### Authors' contributions

Study design: SA and PB; Data collection, analysis, interpretation and manuscript preparation SA, RB, XS, SD, LtenB, DdeW; Critical appraisal, manuscript review and editing JV, GR, ROE, UB, CP, PB; Funding acquisition: PB.

### Acknowledgements

The AAV8 expression cassette used for these experiments was kindly provided by Dr. F. Mingozzi, Généthon, Evry, France.

### Supplementary data

Supplementary data to this article can be found online at <https://doi.org/10.1016/j.jhep.2019.03.021>.

### References

Author names in bold designate shared co-first authorship

- [1] Reichert MC, Lammert F. *ABCB4* gene aberrations in human liver disease: an evolving spectrum. *Semin Liver Dis* 2018;38: 299–307.
- [2] Alissa FT, Jaffe R, Shneider BL. Update on progressive familial intrahepatic cholestasis. *J Pediatr Gastroenterol Nutr* 2008;46:241–252.
- [3] Jacquemin E, De Vree JM, Cresteil D, Sokal EM, Sturm E, Dumont M, et al. The wide spectrum of multidrug resistance 3 deficiency: from neonatal cholestasis to cirrhosis of adulthood. *Gastroenterology* 2001;120:1448–1458.
- [4] de Vree JM, Jacquemin E, Sturm E, Cresteil D, Bosma PJ, Aten J, et al. Mutations in the *MDR3* gene cause progressive familial intrahepatic cholestasis. *Proc Natl Acad Sci U S A* 1998;95:282–287.
- [5] van Helvoort A, Smith AJ, Sprong H, Fritzsche I, Schinkel AH, Borst P, et al. *MDR1* P-glycoprotein is a lipid translocase of broad specificity, while *MDR3* P-glycoprotein specifically translocates phosphatidylcholine. *Cell* 1996;87:507–517.
- [6] Davit-Spraul A, Gonzales E, Baussan C, Jacquemin E. The spectrum of liver diseases related to *ABCB4* gene mutations: pathophysiology and clinical aspects. *Semin Liver Dis* 2010;30:134–146.
- [7] Smit JJ, Schinkel AH, Oude Elferink RP, Groen AK, Wagenaar E, van Deemter L, et al. Homozygous disruption of the murine *mdr2* P-glycoprotein gene leads to a complete absence of phospholipid from bile and to liver disease. *Cell* 1993;75:451–462.
- [8] Jacquemin E, Hermans D, Myara A, Habes D, Debray D, Hadchouel M, et al. Ursodeoxycholic acid therapy in pediatric patients with progressive familial intrahepatic cholestasis. *Hepatology* 1997;25:519–523.
- [9] Beuers U, Trauner M, Jansen P, Poupon R. New paradigms in the treatment of hepatic cholestasis: from UDCA to FXR, PXR and beyond. *J Hepatol* 2015;62:S25–37.
- [10] Lemoine C, Bhardwaj T, Bass LM, Superina RA. Outcomes following partial external biliary diversion in patients with progressive familial intrahepatic cholestasis. *J Pediatr Surg* 2017;52:268–272.
- [11] Erginel B, Soysal FG, Durmaz O, Celik A, Salman T. Long-term outcomes of six patients after partial internal biliary diversion for progressive familial intrahepatic cholestasis. *J Pediatr Surg* 2018;53:468–471.
- [12] Mehl A, Bohorquez H, Serrano MS, Galliano G, Reichman TW. Liver transplantation and the management of progressive familial intrahepatic cholestasis in children. *World J Transplant* 2016;6:278–290.
- [13] Englert C, Grabhorn E, Richter A, Rogiers X, Burdelski M, Ganschow R. Liver transplantation in children with progressive familial intrahepatic cholestasis. *Transplantation* 2007;84:1361–1363.
- [14] Nathwani AC, Reiss UM, Tuddenham EG, Rosales C, Chowdary P, McIntosh J, et al. Long-term safety and efficacy of factor IX gene therapy in hemophilia B. *N Engl J Med* 2014;371:1994–2004.
- [15] Collaud F, Bortolussi G, Guianvarc'h L, Aronson SJ, Bordet T, Veron P, et al. Preclinical development of an AAV8-hUGT1A1 vector for the treatment of Crigler-Najjar syndrome. *Mol Ther Methods Clin Dev* 2018;12:157–174.
- [16] Ferla R, Alliegro M, Marteau JB, Dell'Anno M, Nusco E, Pouillot S, et al. Non-clinical safety and efficacy of an AAV2/8 vector administered intravenously for treatment of mucopolysaccharidosis type VI. *Mol Ther Methods Clin Dev* 2017;6:143–158.
- [17] Puzzo F, Colella P, Biferi MG, Bali D, Paulk NK, Vidal P, et al. Rescue of Pompe disease in mice by AAV-mediated liver delivery of secreted acid alpha-glucosidase. *Sci Transl Med* 2017;9.
- [18] Mingozzi F, High KA. Therapeutic in vivo gene transfer for genetic disease using AAV: progress and challenges. *Nat Rev Genet* 2011;12:341–355.
- [19] Cunningham SC, Dane AP, Spinoulas A, Logan GJ, Alexander IE. Gene delivery to the juvenile mouse liver using AAV2/8 vectors. *Mol Ther* 2008;16:1081–1088.

- [20] Wang Z, Zhu T, Qiao C, Zhou L, Wang B, Zhang J, et al. Adeno-associated virus serotype 8 efficiently delivers genes to muscle and heart. *Nat Biotechnol* 2005;23:321–328.
- [21] Bortolussi G, Zentillin L, Vaniikova J, Bockor L, Bellarosa C, Mancarella A, et al. Life-long correction of hyperbilirubinemia with a neonatal liver-specific AAV-mediated gene transfer in a lethal mouse model of Crigler-Najjar Syndrome. *Hum Gene Ther* 2014;25:844–855.
- [22] Mingozzi F, High KA. Overcoming the host immune response to adeno-associated virus gene delivery vectors: the race between clearance, tolerance, neutralization, and escape. *Annu Rev Virol* 2017;4:511–534.
- [23] Mauad TH, van Nieuwkerk CM, Dingemans KP, Smit JJ, Schinkel AH, Notenboom RG, et al. Mice with homozygous disruption of the *mdr2* P-glycoprotein gene. A novel animal model for studies of nonsuppurative inflammatory cholangitis and hepatocarcinogenesis. *Am J Pathol* 1994;145:1237–1245.
- [24] Oude Elferink RP, Ottenhoff R, van Wijland M, Smit JJ, Schinkel AH, Groen AK. Regulation of biliary lipid secretion by *mdr2* P-glycoprotein in the mouse. *J Clin Invest* 1995;95:31–38.
- [25] Smith AJ, de Vree JM, Ottenhoff R, Oude Elferink RP, Schinkel AH, Borst P. Hepatocyte-specific expression of the human MDR3 P-glycoprotein gene restores the biliary phosphatidylcholine excretion absent in *Mdr2*<sup>-/-</sup> mice. *Hepatology* 1998;28:530–536.
- [26] Van Nieuwkerk CM, Elferink RP, Groen AK, Ottenhoff R, Tytgat GN, Dingemans KP, et al. Effects of Ursodeoxycholate and cholate feeding on liver disease in FVB mice with a disrupted *mdr2* P-glycoprotein gene. *Gastroenterology* 1996;111:165–171.
- [27] Mingozzi F, Liu YL, Dobrzynski E, Kaufhold A, Liu JH, Wang Y, et al. Induction of immune tolerance to coagulation factor IX antigen by in vivo hepatic gene transfer. *J Clin Invest* 2003;111:1347–1356.
- [28] Miao CH, Ohashi K, Patijn GA, Meuse L, Ye X, Thompson AR, et al. Inclusion of the hepatic locus control region, an intron, and untranslated region increases and stabilizes hepatic factor IX gene expression in vivo but not in vitro. *Mol Ther* 2000;1:522–532.
- [29] Matsushita T, Elliger S, Elliger C, Podsakoff G, Villarreal L, Kurtzman GJ, et al. Adeno-associated virus vectors can be efficiently produced without helper virus. *Gene Ther* 1998;5:938–945.
- [30] Wu Z, Yang H, Colosi P. Effect of genome size on AAV vector packaging. *Mol Ther* 2010;18:80–86.
- [31] Scheffer GL, Kool M, Heijn M, de Haas M, Pijnenborg AC, Wijnholds J, et al. Specific detection of multidrug resistance proteins MRP1, MRP2, MRP3, MRP5, and MDR3 P-glycoprotein with a panel of monoclonal antibodies. *Cancer Res* 2000;60:5269–5277.
- [32] Nicolson SC, Li C, Hirsch ML, Setola V, Samulski RJ. Identification and validation of small molecules that enhance recombinant adeno-associated virus transduction following high-throughput screens. *J Virol* 2016;90:7019–7031.
- [33] Montecucco A, Zanetta F, Biamonti G. Molecular mechanisms of etoposide. *EXCLI J* 2015;14:95–108.
- [34] **Slijepcevic D, Roscam Abbing RLP**, Fuchs CD, Haazen LCM, Beuers U, Trauner M, et al. Na(+)-taurocholate cotransporting polypeptide inhibition has hepatoprotective effects in cholestasis in mice. *Hepatology* 2018, [Epub ahead of print].
- [35] Paulusma CC, Groen A, Kunne C, Ho-Mok KS, Spijkerboer AL, Rudi de Waart D, et al. *Atp8b1* deficiency in mice reduces resistance of the canalicular membrane to hydrophobic bile salts and impairs bile salt transport. *Hepatology* 2006;44:195–204.
- [36] Slijepcevic D, Roscam Abbing RLP, Katafuchi T, Blank A, Donkers JM, van Hoppe S, et al. Hepatic uptake of conjugated bile acids is mediated by both sodium taurocholate cotransporting polypeptide and organic anion transporting polypeptides and modulated by intestinal sensing of plasma bile acid levels in mice. *Hepatology* 2017;66:1631–1643.
- [37] Montenegro-Miranda PS, Pichard V, Aubert D, Ten Bloemendaal L, Duijst S, de Waart DR, et al. In the rat liver, adenoviral gene transfer efficiency is comparable to AAV. *Gene Ther* 2014;21:168–174.
- [38] Seppen J, van Til NP, van der Rijt R, Hiralall JK, Kunne C, Elferink RP. Immune response to lentiviral bilirubin UDP-glucuronosyltransferase gene transfer in fetal and neonatal rats. *Gene Ther* 2006;13:672–677.
- [39] James J, Bosch KS, Aronson DC, Houtkooper JM. Sirius red histophotometry and spectrophotometry of sections in the assessment of the collagen content of liver tissue and its application in growing rat liver. *Liver* 1990;10:1–5.
- [40] Standish RA, Cholongitas E, Dhillon A, Burroughs AK, Dhillon AP. An appraisal of the histopathological assessment of liver fibrosis. *Gut* 2006;55:569–578.
- [41] De Vree JM, Ottenhoff R, Bosma PJ, Smith AJ, Aten J, Oude Elferink RP. Correction of liver disease by hepatocyte transplantation in a mouse model of progressive familial intrahepatic cholestasis. *Gastroenterology* 2000;119:1720–1730.
- [42] van der Loos CM, de Boer OJ, Mackaaij C, Hoekstra LT, van Gulik TM, Verheij J. Accurate quantitation of Ki67-positive proliferating hepatocytes in rabbit liver by a multicolor immunohistochemical (IHC) approach analyzed with automated tissue and cell segmentation software. *J Histochem Cytochem* 2013;61:11–18.
- [43] Lammert F, Wang DQ, Hillebrandt S, Geier A, Fickert P, Trauner M, et al. Spontaneous cholecysto- and hepatolithiasis in *Mdr2*<sup>-/-</sup> mice: a model for low phospholipid-associated cholelithiasis. *Hepatology* 2004;39:117–128.
- [44] Choi M, Moschetta A, Bookout AL, Peng L, Umetani M, Holmstrom SR, et al. Identification of a hormonal basis for gallbladder filling. *Nat Med* 2006;12:1253–1255.
- [45] Ziol M, Barbu V, Rosmorduc O, Frassati-Biaggi A, Barget N, Hermelin B, et al. ABCB4 heterozygous gene mutations associated with fibrosing cholestatic liver disease in adults. *Gastroenterology* 2008;135:131–141.
- [46] Sobrevals L, Enguita M, Rodriguez C, Gonzalez-Rojas J, Alzaguren P, Razquin N, et al. AAV vectors transduce hepatocytes in vivo as efficiently in cirrhotic as in healthy rat livers. *Gene Ther* 2012;19:411–417.
- [47] Ehrhardt A, Xu H, Kay MA. Episomal persistence of recombinant adenoviral vector genomes during the cell cycle in vivo. *J Virol* 2003;77:7689–7695.
- [48] Takahashi S, Fukami T, Masuo Y, Brocker CN, Xie C, Krausz KW, et al. *Cyp2c70* is responsible for the species difference in bile acid metabolism between mice and humans. *J Lipid Res* 2016;57:2130–2137.
- [49] **Meliani A, Boisgerault F**, Hardet R, Marmier S, Collaud F, Ronzitti G, et al. Antigen-selective modulation of AAV immunogenicity with tolerogenic rapamycin nanoparticles enables successful vector re-administration. *Nat Commun* 2018;9:4098.